Received: 6 June 2016 | Revised: 12 March 2017 | Accepted: 22 March 2017
DOI: 10.1111/ter.12265

PAPER

WILEY Terra Nova

Phanerozoic magma underplating and crustal growth beneath the North China Craton

Qiang Ma[1] | Yi-Gang Xu[1] | Jian-Ping Zheng[2] | Min Sun[3] | William L. Griffin[4] | Xiaoping Xia[1] | Shao-Kui Pan[2]

[1]State Key Laboratory of Isotope Geochemistry, Guangzhou Institute of Geochemistry, Chinese Academy of Sciences, Guangzhou, China

[2]State Key Laboratory of Geological Processes and Mineral Resources, School of Earth Sciences, China University of Geosciences, Wuhan, China

[3]Department of Earth Sciences, The University of Hong Kong, Hong Kong, China

[4]ARC CoE for Core to Crust Fluid Systems/GEMOC, Macquarie University, Sydney, NSW, Australia

Correspondence
Qiang Ma, State Key Laboratory of Isotope Geochemistry, Guangzhou Institute of Geochemistry, Chinese Academy of Sciences, Guangzhou, China.
Emails: maqiang@gig.ac.cn; maqiang32@126.com

Funding information
DREAM project of the Ministry of Science and Technology of China, Grant/Award Number: 2016YFC0600403; 2016YFC0600103; Research Project of the State Oceanic Administration of China, Grant/Award Number: GASI-GEOGE-02; National Natural Science Foundation of China, Grant/Award Number: 41502040

Abstract

Evidence for post-Archaean crustal growth via magma underplating is largely based on U–Pb dating of zircons from granulite-facies xenoliths. However, whether the young zircons from such xenoliths are genetically related to magma underplating or to anatexis remains controversial. The lower-crustal xenoliths carried by igneous rocks in the Chifeng and Ningcheng (North China Craton) have low SiO_2 and high MgO, indicating that parental melts of their protoliths were of unambiguous mantle origin. The xenoliths contain abundant magmatic zircons with late-Palaeozoic ages, and have more radiogenic zircon Hf-isotope compositions and hence younger model ages than ancient crustal magmas and the "reworking array" of the basement rocks. Our data suggest that the granulites represent episodic magmatic underplating to the lower crust of this craton in Phanerozoic time. Considering the observation that regional lowermost crust (~5 km) is mafic and characterized by Phanerozoic zircons, this work reports an example of post-Archaean crustal growth via magma underplating.

1 | INTRODUCTION

Underplating of magmas is an efficient mechanism for generating lower continental crust (Hacker, Kelemen & Behn, 2015; Hawkesworth & Kemp, 2006a; Rudnick, 1995). This has been exemplified by lower-crustal granulite xenoliths that contain zircons with younger ages than the exposed basement rocks (Davis, 1997; Moyen et al., 2017). For example, Phanerozoic zircons (45–220 Ma) have been reported in granulite xenoliths from the Cenozoic basalts in the Hannuoba area of the North China Craton (NCC) (Fan et al., 1998; Liu et al., 2004; Wei, Zheng, Su, Ma & Griffin, 2015; Zheng et al., 2009). These ages are obviously younger than those of the rocks of the nearby exposed Archaean granulite terrane, and have been regarded as strong evidence for Phanerozoic underplating underneath Archaean cratons. However, some Archaean zircons are also preserved in the Hannuoba granulite xenoliths, and the Mesozoic zircons have unradiogenic Hf-isotope compositions, apparently implying reworking of pre-existing Archaean lower crust rather than the creation of new crust. This may suggest an alternative interpretation, i.e. the young zircons were generated during high-grade metamorphism and crustal anatexis rather than crystallized in underplated magmas (Jiang & Guo, 2010; Wilde, Zhou, Nemchin & Sun, 2003). Therefore, deciphering the significance of young zircons from granulite xenoliths is important to understanding post-Archaean underplating and crustal growth.

Metamorphic zircons are generally associated with the reworking process. Magmatic zircons crystallized during anatexis of pre-existing crust are characterized by unradiogenic Hf-isotope compositions, consistent with those of the basement rocks. In contrast, zircons crystallized from underplated magmas would have Hf-isotope compositions consistent with the melting depleted or enriched mantle source (Couzinié et al., 2016), which generally is distinct from the basement rocks. In this work, integrated studies of internal structure, U–Pb and Hf-isotope analyses were carried out on zircons from lower-crustal xenoliths in the early Mesozoic Chifeng and Ningcheng igneous rocks (Figure 1), ~250–350 km northeast of Hannuoba, with the aim of testing whether the young zircons from these deep-crustal xenoliths record Phanerozoic underplating beneath the ancient NCC.

2 | GEOLOGICAL SETTING AND SAMPLES

The NCC is one of the oldest Archaean cratons in the world and preserves ≥3.8 Ga crustal remnants (Liu, Nutman, Compston, Wu & Shen, 1992). Crustal growth in the NCC occurred as early as ~4.0–3.9 Ga and reached its climax at ~2.8–2.5 Ga (Geng, Du & Ren, 2012; Wu, Zhao, Wilde & Sun, 2005; Zheng et al., 2012). The Archaean crust was re-worked when the Western and Eastern Blocks amalgamated to form a united NCC in the late Palaeoproterozoic (~1.9–1.8 Ga) (Geng et al., 2012; Zheng et al., 2012). This craton was reactivated and lost much of its lithospheric keel (>100 km) in the Mesozoic (Griffin, Zhang, O'Reilly & Ryan, 1998; Menzies, Fan & Zhang, 1993). Consequently, Mesozoic igneous rocks with abundant granulite-facies xenoliths are widespread (Figure 1) and provide direct samples of the deep crust of the NCC. The Ningcheng and Chifeng igneous complexes were emplaced at mid- to lower-crustal depths (~4.9–8.3 kbar; Ma, Xu, Zheng, Sun et al., 2016) in the early Mesozoic (~227 Ma). The Ningcheng complex preserves a fractionating system, consisting of cumulates and residual melts from hydrous mafic magmas, derived from an enriched mantle (Ma, Xu, Zheng, Sun et al., 2016). Petrogenesis of the Chifeng gabbroic diorites is not well constrained, but their geochemical compositions also suggest an origin from an enriched mantle source (She et al., 2006). The diorites and gabbroic diorites carry abundant enclaves, including two-pyroxene granulites, clinopyroxene (Cpx) granulites, Cpx-amphibolites and metagabbros. Petrography and *P*–*T* estimates reveal that they are lower-crustal xenoliths rather than co-magmatic enclaves (Shao & Wei, 2011). The samples investigated here include five mafic two-pyroxene (2-Py) granulites (NC1101, NC1102, NCH1205, CF1108 and CF1202), one Cpx-granulite (CF1211), two Cpx-amphibolites (CF1106 and CF1113) (Table 1) and two host rocks (NC1140 and CF1114). The xenoliths are angular to rounded (~8–20 cm in diameter) and contain granoblastic assemblages of Cpx, orthopyroxene (Opx) and plagioclase (Pl) with variable amounts of amphibole (Am) (see Figure S1).

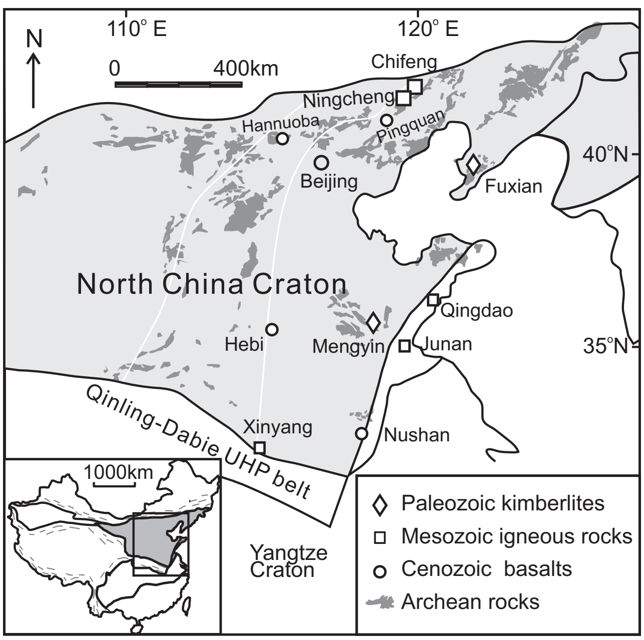

FIGURE 1 Geological sketch map showing outcropping Archaean rocks and localities with lower-crustal xenoliths in Phanerozoic igneous rocks in the NCC [Colour figure can be viewed at wileyonlinelibrary.com]

3 | METHODS

Major-element compositions of whole rocks and of minerals were measured by XRF and EPMA, respectively. Details of the measurement procedure and data quality are provided in the annotations of Tables S1 and S2.

All the analyses on zircons were conducted at Guangzhou Institute of Geochemistry, Chinese Academy of Sciences. Cathodoluminescence (CL) images of zircon were obtained prior to SIMS analysis, using a Supra 55 Sapphire FE-SEM. SIMS analyses of U–Pb isotopes of zircon were performed on a Cameca IMS 1280-HR ion microprobe following procedures described by Li, Liu, Li, Guo and Chamberlain (2009). The O_2^- primary ion beam was accelerated at 13 kV, with an intensity of 10 nA. The ellipsoidal spot is about 20 × 30 μm in size. Positive secondary ions were extracted with a 10 kV potential. Calibration of Pb/U ratios is based on an observed linear relationship between $\ln(^{206}Pb/^{238}U)$ and $\ln(^{238}U^{16}O_2/^{238}U)$. A common-Pb correction was applied using the measured ^{204}Pb. Zircon Plesovice was used as an external standard for U–Pb dating, and zircon standard Qinghu was used to monitor the measurement procedure and data quality. Zircon Lu–Hf isotope analyses were conducted using a Neptune Plus MC-ICP-MS in combination with a RESOlution M-50 laser ablation system, with a beam diameter of 45 μm. Zircon standard Penglai was used to monitor the measurement procedures and data quality. All the analytical results are listed in Tables S1–S3.

4 | RESULTS AND INTERPRETATIONS OF ZIRCON U–PB AND LU–HF DATA

Most zircons from the host rocks (Ningcheng diorite NC1140 and Chifeng gabbroic diorite CF1114) are euhedral and show oscillatory

TABLE 1 Summary of P–T conditions and zircon ages of lower-crustal xenoliths from early Mesozoic plutons in the northern NCC

Sample[a]	Lithology	SiO_2 (wt%)	T-W (°C)	T-WB (°C)	P-HZ (kbar)	Magmatic age	Metamorphic age
NC1101	2-Py granulite	50.4	982	924	7.3	~312 Ma	~224 Ma
NC1102	2-Py granulite	51.2	912	870	7.5	~1,856 Ma ~320 Ma	~227 Ma
NCH1205	2-Py granulite	48.9	890	865	8.0	~318 Ma	~233 Ma
CF1106	Cpx-Amphibolite	48.7				~260 Ma	n/a
CF1108	2-Py granulite	49.3	911	875	7.8	~261 Ma	n/a
CF1113	Cpx-Amphibolite	46.3	913	898	6.7	~260 Ma	n/a
CF1202	2-Py granulite	51.0				~2,518 Ma[b] ~259 Ma	n/a
CF1211	Cpx granulite	50.3				~258 Ma	n/a
SW	Granulites		*T* = 807~1,104°C		*P* = 10 kbar		

T-W and T-WB: thermometers from Wells (1997) and Wood and Banno (1973), respectively.
P-HZ: barometer from McCarthy and Patiño Douce (1998).
[a]NC is Ningcheng; CF is Chifeng; SW is samples from Shao and Wei (2011).
[b]Inherited cores.

zoning in CL images (Figures S2–S3), indicating crystallization from magmas. They yield weighted mean $^{206}Pb/^{238}U$ ages of 227.4 ± 2.1 Ma for those from sample NC1140 and 228.2 ± 3.1 Ma for those from sample CF1114, respectively, which are interpreted as the crystallization ages of the plutons. These zircons have a restricted range of Hf-isotope compositions ($\varepsilon_{Hf}(t)$ = −2.1 to +1.2; Figure 2). Inherited irregular zircon grains with oscillatory zoning are observed in sample CF1114 and yield a weighted mean $^{206}Pb/^{238}U$ age of 261.7 ± 2.6 Ma. They have less-radiogenic Hf-isotope compositions than the Triassic grains ($\varepsilon_{Hf}(t)$ = −18.5 to −15.1; Figure 2), indicating they are xenocrysts.

CL images of zircons from the mafic xenoliths show core–rim structures with oscillatorily zoned magmatic cores surrounded by narrow light and unzoned metamorphic rims (Figures 2, S2 and S3). *Ningcheng zircons*: The cores of zircons in NC1102 yield an upper intercept U–Pb age of ~1856 Ma, and they are surrounded by metamorphic rims of late Triassic age (~227 Ma). Some grains from this granulite also show core–mantle–rim structures with magmatic mantles of late Palaeozoic age (~320 Ma). The Palaeoproterozoic cores have chondrite-like Hf-isotopic compositions with $\varepsilon_{Hf}(t)$ of −2.7 to +0.2 (Figure 2a). In contrast, the Phanerozoic mantles and rims have unradiogenic isotopic compositions with $\varepsilon_{Hf}(t)$ of −13.2 to −7.5 and −23.6 to −19.2, respectively. The zircons in NC1101 and NCH1205 have similar ages, with ~315 Ma cores and ~223 Ma rims (Figure S2), and the cores and rims have identical Hf isotopes ($\varepsilon_{Hf}(t)$ = −10.2 to −2.3; Figures 2a and S4). *Chifeng zircons*: All the zircon cores from the Chifeng xenoliths have similar ages of ~260 Ma (Figure S3) and $\varepsilon_{Hf}(t)$ values from −21.2 to −4.2 (Figures 2 and S5). Two Neoarchaean (~2518 Ma) inherited cores in CF1202 have $\varepsilon_{Hf}(t)$ of +1.2 and +4.4. The rims of zircons from Chifeng xenoliths are generally too narrow for SIMS U–Pb dating.

The morphology and ages of these zircons indicate that the protoliths of these high-grade metamorphic rocks formed at ~1856 Ma (NC1102), ~315 Ma (NC1101 and NCH1205) and ~260 Ma (CF1106, CF1108, CF1113, CF1202 and CF1211), and all experienced metamorphism in the late Triassic (*ca* 230 Ma).

5 | DISCUSSION

5.1 | Petrogenesis of the xenoliths

The Chifeng and Ningcheng granulites and amphibolites are considered to be lower-crustal xenoliths on the basis of the following observations:

1. They are angular to rounded and show sharp contacts with the host plutons (Figure S1).
2. U–Pb dating of zircon cores from these enclaves yields three main distinct age populations of ~1.85 Ga, ~315 Ma and ~260 Ma, which are significantly older than the emplacement time of their host igneous rocks (~227 Ma).
3. Zircons from the host plutons and enclaves have different Hf-isotope compositions (Figure 2).
4. The studied xenoliths record equilibration temperatures from 865 to 982°C and pressures from 6.7 to 8.0 kbar, corresponding to depths of 22–26 km (Table 1).

The lower-crustal xenoliths have basaltic compositions with low SiO_2 (~46.3%–51.3%) and high MgO (~4.4%–7.8%) and Fe_2O_3 (~9.1%–15.7%), which demonstrates that parental melts of their protoliths were unequivocally derived from an ultramafic mantle rather than from crustal lithologies (Figure 3). Most zircons in these mafic lower-crustal xenoliths (except NC1102) are characterized by Phanerozoic (~321–255 Ma) magmatic cores surrounded by 218–241 Ma metamorphic/recrystallized rims. Moreover, the Hf isotopes of the magmatic zircons are consistent with those of contemporary mantle-derived magmas in the NCC (Figure 2). Thus, we propose that these mafic rocks represent late-Palaeozoic underplated basaltic magmas (with or without crustal assimilation) which were later subjected to amphibolite- to granulite-facies metamorphism. Two-pyroxene granulite NC1102 contains zircons with Palaeoproterozoic (~1,856 Ma) magmatic cores and late Triassic rims. Both the magmatic cores and the metamorphic rims have unradiogenic Hf

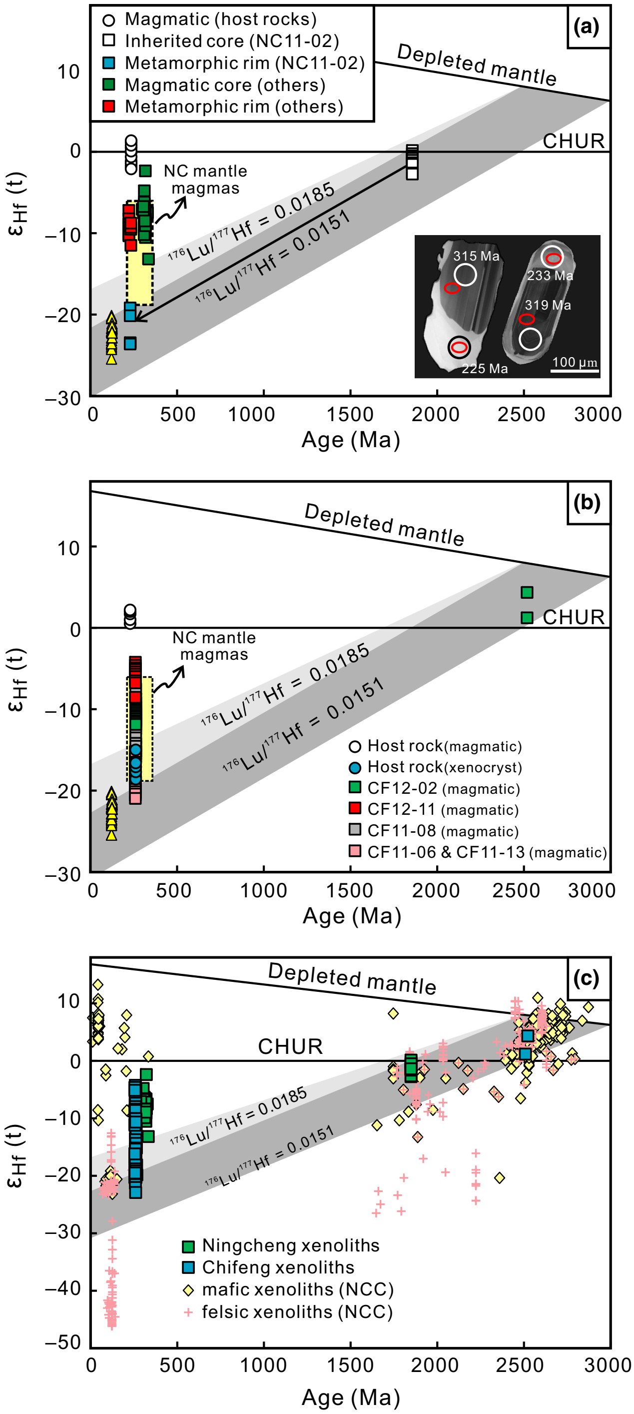

FIGURE 2 Plots of zircon $\varepsilon_{Hf}(t)$ vs. U–Pb age for lower-crustal xenoliths from (a) Ningcheng, (b) Chifeng and (c) other Phanerozoic igneous rocks in the NCC. The $^{176}Lu/^{177}Hf$ ratios (0.0151 and 0.0185) and reworking arrays of Precambrian basement of the NCC are derived by regression through the zircons in granulite NC1102 and in ancient lower crust and their melts (Figure S6). The light-yellow field represents Palaeozoic mantle-derived magmas in the northern NCC (Figure S4). The yellow triangles in (a) and (b) represent Mesozoic magmas derived from ancient lower crust in the NCC (Ma, Xu, Zheng, Griffin et al., 2016; Yang et al., 2007). Data sources for zircons in lower-crustal xenoliths from other places in (c) are listed in Data S1 [Colour figure can be viewed at wileyonlinelibrary.com]

isotopes ($\varepsilon_{Hf}(t)$ = −2.7 to +0.2 and −23.6 to −19.2, respectively) that are consistent with those of zircons from the Archaean lower crust beneath the NCC (Figure S4). These data suggest that the protolith of this granulite was formed at ~1.85 Ga by reworking of Archaean crust and suffered further metamorphism in the late Triassic. Rare magmatic mantles with late Palaeozoic ages and less unradiogenic Hf isotopes (Figure S4c) suggest the lower crust may also been affected by the late Palaeozoic thermal event.

5.2 | Significance of unradiogenic zircon Hf-isotopic compositions

Zircons with Mesozoic ages have been identified in many of the granulite xenoliths in the NCC and are inferred to be an indicator of post-Archaean underplating beneath cratons (Zhang et al., 2013). An alternative petrogenetic model for these xenoliths suggests that the young zircons (re-)crystallized during high-grade metamorphism and crustal anatexis/reworking (Jiang & Guo, 2010; Wilde et al., 2003). This reworking model is mainly built on three lines of evidence: (1) the morphology of young zircons, suggestive of a metamorphic origin, (2) the preservation of Precambrian zircon grains and (3) the unradiogenic Hf isotopes of the late Mesozoic zircons.

As demonstrated in the previous section, only a single sample from our dataset (NC1102) shows evidence for reworking of Palaeoproterozoic lower crust. Other samples from both localities represent late Palaeozoic/early Mesozoic underplated mafic magmas containing well-developed, oscillatorily zoned and clearly igneous zircons. The unradiogenic Hf isotopes of these zircons (Figure 2) did not result from crustal contamination, because this scenario needs a huge amount of contamination to reach such negative ε_{Hf}, such that the melts would no longer be mafic. Then, these zircons could accordingly be taken as an indicator of crustal reworking. However, this

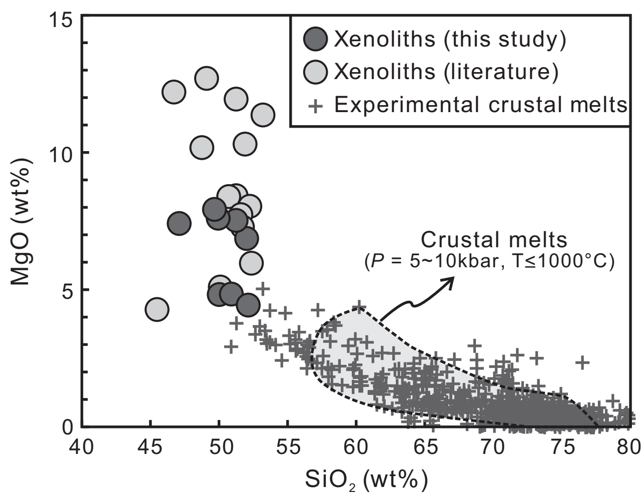

FIGURE 3 Plot of MgO vs. SiO_2 for mafic lower-crustal xenoliths from early Mesozoic plutons in the northern part of the NCC. Data sources: lower-crustal xenoliths are from Shao, Han and Li (2000), Shao, Zhang, She and Liu (2012) and this study; experimental melts from crustal rocks are compiled from Gao, Zheng and Zhao (2016)

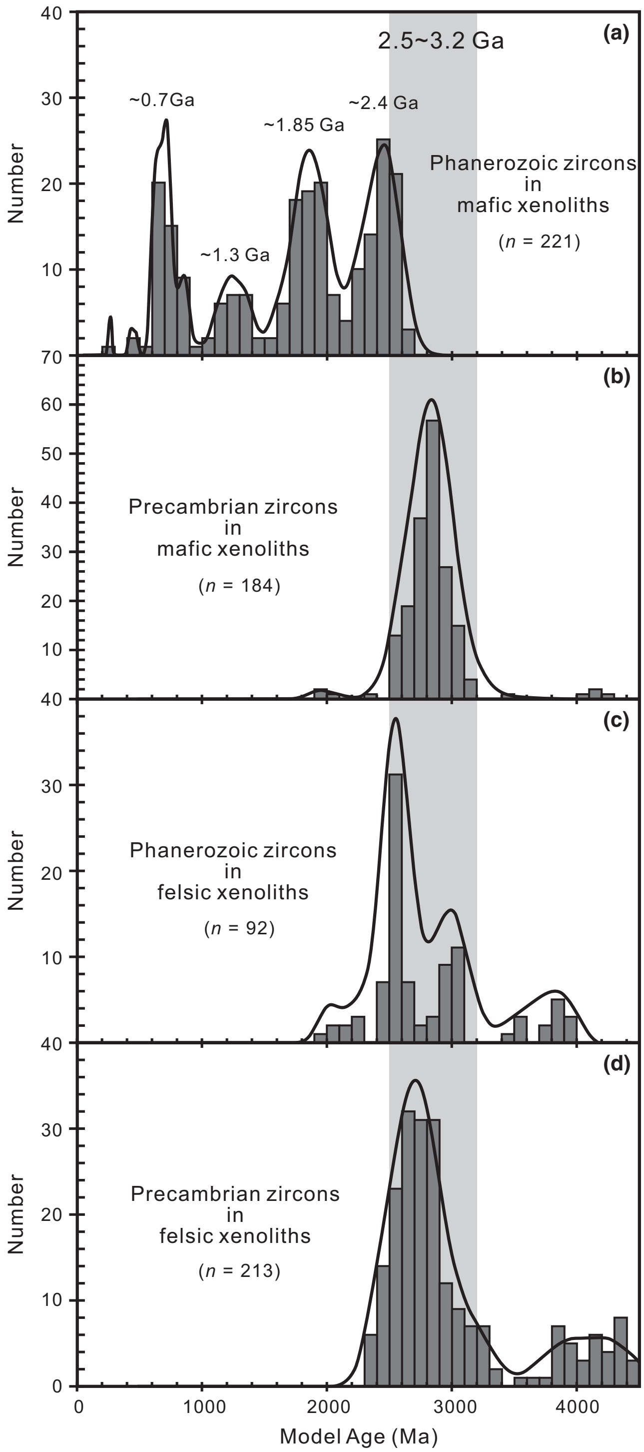

FIGURE 4 Histograms of Hf model ages of magmatic zircons from mafic (a–b) and felsic (c–d) lower-crustal xenoliths in the NCC (data sources as in Figure 2). The grey field represents the major stage of crustal formation of the NCC during Precambrian times, as estimated from relative areas of outcropping crust

hypothesis relies on the paradigm that zircons crystallized during anatexis of pre-existing ancient crust have unradiogenic Hf-isotope compositions, whereas zircons crystallized in mantle melts have radiogenic Hf-isotopes similar to contemporary depleted mantle (Hawkesworth & Kemp, 2006b; Yang, Wu, Wilde, Belousova & Griffin, 2008). Recently, the reliability of this paradigm has been questioned (Laurent & Zeh, 2015; Payne et al., 2016; Vervoort & Kemp, 2016). Here, we investigate the meaning of the unradiogenic zircon Hf isotopes of the Ningcheng and Chifeng xenoliths by using their deviation from the basement rocks rather than from CHUR or depleted mantle. We have constructed the "reworking array" of the regional Precambrian basement using the zircon Hf isotopes of granulite NC1102 (which formed by reworking of Palaeoproterozoic lower crust, as discussed before) and of ancient lower crust and their melts (Figures 2 and S6). As shown in Figure 2, except for some grains from the Chifeng xenoliths, most Phanerozoic magmatic zircons in the studied lower-crustal xenoliths and their host rocks have more radiogenic Hf isotopes (higher $\varepsilon_{Hf}(t)$ values) than the regional basement, suggesting that they are unlikely to have been derived by reworking or assimilation of that basement.

5.3 | Accretion of lower crust by magmatic underplating

New crust or underplating magmas can be derived not only from depleted mantle but also from enriched mantle sources. In the latter case, magmatic zircons could have "crust-like" unradiogenic Hf-isotope composition (e.g. Couzinié et al., 2016). Phanerozoic mafic magmas, caused by destruction of cratonic lithosphere, were widespread in the NCC and were largely derived from enriched mantle before ~100 Ma (Huang, Zhong & Xu, 2012; Xu, Li, Pang & He, 2009). The Hf-isotope compositions of the late Palaeozoic magmatic zircons in the Ningcheng and Chifeng xenoliths are consistent with those of zircons crystallized from regional contemporary mafic magmas, which derived from an enriched mantle that had previously been metasomatized by crustal components. Therefore, we argue that the young (younger than the basement) magmatic zircons from the xenoliths are genetically related to Phanerozoic magma underplating beneath the lower crust rather than to anatexis. It has been demonstrated that the lowermost crust (~5 km) of the northern NCC is mafic and contains zircons with Phanerozoic ages (e.g. Liu et al., 2001; Wei et al., 2015; Zhang et al., 2013). Here we demonstrate that the protoliths of these lower-crustal rocks were formed by Phanerozoic magma underplating. Consequently, such magmatism could represent significant additions to crustal growth.

Underplated magmas at the base of the crust could be basaltic in composition and may have reworked the pre-existing ancient lower crust by heating and rehydration. As shown in Figure 2c, Phanerozoic magmatic zircons from felsic lower-crustal xenoliths have Hf isotopes comparable to those of Archaean lower crust beneath the NCC, but are less radiogenic than those from mafic xenoliths. Depleted-mantle Hf model ages are used to further elucidate the difference between the mafic and felsic xenoliths. In order to lessen the problem of calculating depleted-mantle model ages (Payne et al., 2016), $^{176}Lu/^{177}Hf = 0.0151$ is assigned to the nominal protolith source based on the regression through zircons in granulite NC1102 (Figure S6). It should be noted that these model ages may not represent the true time of crust generation (Nebel,

Nebel-Jacobsen, Mezger & Berndt, 2007; Vervoort & Kemp, 2016), but are useful for examining differences between populations. The depleted-mantle Hf model ages of magmatic zircons from the Phanerozoic mafic lower crust define four populations at ~2.4 Ga, ~1.85 Ga, ~1.3 Ga and ~0.7 Ga, which are distinct from the model-age patterns of both pre-existing Archaean–Proterozoic crust (Figure 4) and Phanerozoic magmatic zircons from felsic lower-crustal xenoliths. It is clear that some of the young zircons from mafic lower-custal xenoliths bear witness to Phanerozoic crustal growth by magma underplating in the NCC. In contrast, most of the intermediate–felsic granulites with young zircons were generated by reworking of ancient lower crust via heating, probably from the underplated mafic magmas.

6 | CONCLUDING REMARKS

1. Protoliths of the Chifeng and Ningcheng lower-crustal xenoliths represent mantle-derived melts. Although they have unradiogenic Hf-isotope signatures, zircons from these rocks reflect an enriched-mantle source rather than reworking of the Precambrian basement.
2. Lower-crustal xenoliths carried by igneous rocks in the NCC record episodic Phanerozoic underplating beneath the Archaean cratons. This work reports an example of post-Archaean crustal growth via magma underplating.

ACKNOWLEDGEMENTS

We thank Bin Lei, Qing Yang, Le Zhang and Qunke Xia for help with zircon U–Pb–Hf and silicate chemistry analyses. This paper benefitted greatly from significant and constructive comments from Oscar Laurent, Fuyuan Wu and Klaus Mezger (journal editor). This work was supported by funds from the Ministry of Science and Technology of China (2016YFC0600103 and 2016YFC0600403), the State Oceanic Administration of China (GASI-GEOGE-02) and the NSFC (41502040). This is contribution No.IS-2381 from GIG-CAS, 959 from the ARC Centre of Excellence for Core to Crust Fluid Systems and 1149 from the GEMOC Key Centre.

REFERENCES

Couzinié, S., Laurent, O., Moyen, J., Zeh, A., Bouilhol, P., & Villaros, A. (2016). Post-collisional magmatism: Crustal growth not identified by zircon Hf-O isotopes. *Earth and Planetary Science Letters*, *456*, 182–195.

Davis, W. J. (1997). U-Pb zircon and rutile ages from granulite xenoliths in the Slave province: Evidence for mafic magmatism in the lower crust coincident with Proterozoic dike swarms. *Geology*, *25*, 343–346.

Fan, Q. C., Liu, R. X., Li, H. M., Li, N., Sui, J. L., & Lin, Z. R. (1998). Zircon geochronology and rare earth element geochemistry of granulite xenoliths from Hannuoba. *Chinese Science Bulletin*, *43*, 133–137.

Gao, P., Zheng, Y. F., & Zhao, Z. F. (2016). Experimental melts from crustal rocks: A lithochemical constraint on granite petrogenesis. *Lithos*, *266–267*, 133–157.

Geng, Y., Du, L., & Ren, L. (2012). Growth and reworking of the early Precambrian continental crust in the North China Craton: Constraints from zircon Hf isotopes. *Gondwana Research*, *21*, 517–529.

Griffin, W. L., Zhang, A., O'Reilly, S. Y., & Ryan, C. G. (1998). Phanerozoic evolution of the lithosphere beneath the Sino-Korean Craton. In M. Flower, S. L. Chung, C. H. Lo & T. Y. Lee (Eds.), *Mantle Dynamics and Plate Interactions in East Asia* (Vol. 27, pp. 107–126). Washington: American Geophysical Union.

Hacker, B. R., Kelemen, P. B., & Behn, M. D. (2015). Continental lower crust. *Annual Review of Earth and Planetary Sciences*, *43*, 167–205.

Hawkesworth, C. J., & Kemp, A. I. S. (2006a). Evolution of the continental crust. *Nature*, *443*, 811–817.

Hawkesworth, C. J., & Kemp, A. I. S. (2006b). Using hafnium and oxygen isotopes in zircons to unravel the record of crustal evolution. *Chemical Geology*, *226*, 144–162.

Huang, X. L., Zhong, J. W., & Xu, Y. G. (2012). Two tales of the continental lithospheric mantle prior to the destruction of the North China Craton: Insights from Early Cretaceous mafic intrusions in western Shandong, East China. *Geochimica et Cosmochimica Acta*, *96*, 193–214.

Jiang, N., & Guo, J. H. (2010). Hannuoba intermediate-mafic granulite xenoliths revisited: Assessment of a Mesozoic underplating model. *Earth and Planetary Science Letters*, *293*, 277–288.

Laurent, O., & Zeh, A. (2015). A linear Hf isotope-age array despite different granitoid sources and complex Archean geodynamics: Example from the Pietersburg block (South Africa). *Earth and Planetary Science Letters*, *430*, 326–338.

Li, X. H., Liu, Y., Li, Q. L., Guo, C. H., & Chamberlain, K. R. (2009). Precise determination of Phanerozoic zircon Pb/Pb age by multicollector SIMS without external standardization. *Geochemistry, Geophysics, Geosystems*, *10*, Q04010.

Liu, Y. S., Gao, S., Jin, S. Y., Hu, S. H., Sun, M., Zhao, Z. B., & Feng, J. L., (2001). Geochemistry of lower crustal xenoliths from Neogene Hannuoba Basalt, North China Craton: Implications for petrogenesis and lower crustal composition. *Geochimica et Cosmochimica Acta*, *65*, 2589–2604.

Liu, Y., Gao, S., Yuan, H., Zhou, L., Liu, X., Wang, X., . . . Wang, L. (2004). U-Pb zircon ages and Nd, Sr, and Pb isotopes of lower crustal xenoliths from North China Craton: Insights on evolution of lower continental crust. *Chemical Geology*, *211*, 87–109.

Liu, D. Y., Nutman, A. P., Compston, W., Wu, J. S., & Shen, Q. H. (1992). Remnants of ≥ 3800 Ma crust in the Chinese part of the Sino-Korean craton. *Geology*, *20*, 339–342.

Ma, Q., Xu, Y. G., Zheng, J. P., Griffin, W. L., Hong, L. B., & Ma, L. (2016). Coexisting early Cretaceous high-Mg andesites and adakitic rocks in the North China Craton: The role of water in intraplate magmatism and cratonic destruction. *Journal of Petrology*, *57*, 1279–1308.

Ma, Q., Xu, Y. G., Zheng, J. P., Sun, M., Griffin, W. L., Wei, Y., . . . Yu, X. (2016). High-Mg adakitic rocks and their complementary cumulates formed by hydrous fractionation of mafic magmas in a continental crustal magma chamber. *Lithos*, *260*, 211–224.

McCarthy, T. C., & Patiño Douce, A. E. (1998). Empirical calibration of the silica-Ca-tschermak's-anorthite (SCAn) geobarometer. *Journal of Metamorphic Geology*, *16*, 675–686.

Menzies, M. A., Fan, W. M., & Zhang, M. (1993). Palaeozoic and Cenozoic lithoprobes and the loss of > 120 km of Archaean lithosphere, Sino-Korean craton, China. *Geological Society, London, Special Publications*, *76*, 71–81.

Moyen, J. F., Paquette, J. L., Ionov, D. A., Gannoun, A., Korsakov, A. V., Golovin, A. V., & Moine, B. N. (2017). Paleoproterozoic rejuvenation and replacement of Archaean lithosphere: Evidence from zircon U–Pb dating and Hf isotopes in crustal xenoliths at Udachnaya, Siberian craton. *Earth and Planetary Science Letters*, *457*, 149–159.

Nebel, O., Nebel-Jacobsen, Y., Mezger, K., & Berndt, J. (2007). Initial Hf isotope compositions in magmatic zircon from early Proterozoic rocks from the Gawler Craton, Australia: A test for zircon model ages. *Chemical Geology*, *241*, 23–37.

Payne, J. L., McInerney, D. J., Barovich, K. M., Kirkland, C. L., Pearson, N. J., & Hand, M. (2016). Strengths and limitations of zircon Lu-Hf and O isotopes in modelling crustal growth. *Lithos*, *248–251*, 175–192.

Rudnick, R. L. (1995). Making continental crust. *Nature*, *378*, 571–578.

Shao, J. A., Han, Q. J., & Li, H. M. (2000). Discovery of the Early Mesozoic granulite xenoliths in North China Craton. *Science in China Series D: Earth Sciences*, *43*, 245–252.

Shao, J., & Wei, C. (2011). Petrology and tectonic significance of the early Mesozoic granulite xenoliths from the eastern Inner Mongolia, China. *Science China Earth Sciences*, *54*, 1484–1491.

Shao, J., Zhang, Z., She, H. Q., & Liu, D. S. (2012). The discovery of Phanerozoic granulite in Chifeng area of North China Craton and its implication. *Earth Science Frontiers*, *19*, 188–198.

She, H. Q., Wang, Y. W., Li, Q. H., Zhang, D. Q., Feng, C. Y., & Li, D. X. (2006). The mafic granulite xenoliths and its implications to mineralization in Chaihulanzi gold deposit, Inner Mongolian, China. *Acta Geologica Sinica*, *80*, 863–874.

Vervoort, J. D., & Kemp, A. I. S. (2016). Clarifying the zircon Hf isotope record of crust–mantle evolution. *Chemical Geology*, *425*, 65–75.

Wei, Y., Zheng, J., Su, Y., Ma, Q., & Griffin, W. L. (2015). Lithological and age structure of the lower crust beneath the northern edge of the North China Craton: Xenolith evidence. *Lithos*, *216*, 211–223.

Wells, P. A. (1997). Pyroxene thermometry in simple and complex systems. *Contributions to Mineralogy and Petrology*, *62*, 129–139.

Wilde, S. A., Zhou, X. H., Nemchin, A. A., & Sun, M. (2003). Mesozoic crust-mantle interaction beneath the North China craton: A consequence of the dispersal of Gondwanaland and accretion of Asia. *Geology*, *31*, 817–820.

Wood, B., & Banno, S. (1973). Garnet-orthopyroxene and orthopyroxene-clinopyroxene relationships in simple and complex systems. *Contributions to Mineralogy and Petrology*, *42*, 109–124.

Wu, F. Y., Zhao, G. C., Wilde, S. A., & Sun, D. Y. (2005). Nd isotopic constraints on crustal formation in the North China Craton. *Journal of Asian Earth Sciences*, *24*, 523–545.

Xu, Y. G., Li, H. Y., Pang, C. J., & He, B. (2009). On the timing and duration of the destruction of the North China Craton. *Chinese Science Bulletin*, *54*, 3379–3396.

Yang, J. H., Wu, F. Y., Wilde, S. A., Belousova, E., & Griffin, W. L. (2008). Mesozoic decratonization of the North China block. *Geology*, *36*, 467–470.

Yang, J., Wu, F., Wilde, S., Xie, L., Yang, Y., & Liu, X. (2007). Tracing magma mixing in granite genesis: In situ U-Pb dating and Hf-isotope analysis of zircons. *Contributions to Mineralogy and Petrology*, *153*, 177–190.

Zhang, H., Zhu, R., Santosh, M., Ying, J., Su, B., & Hu, Y. (2013). Episodic widespread magma underplating beneath the North China Craton in the Phanerozoic: Implications for craton destruction. *Gondwana Research*, *23*, 95–107.

Zheng, J. P., Griffin, W. L., Ma, Q., O'Reilly, S. Y., Xiong, Q., Tang, H. Y., . . . Su, Y. P. (2012). Accretion and reworking beneath the North China Craton. *Lithos*, *149*, 61–78.

Zheng, J. P., Griffin, W. L., Qi, L., O'Reilly, S. Y., Sun, M., Zheng, S., . . . Wu, X. L. (2009). Age and composition of granulite and pyroxenite xenoliths in Hannuoba basalts reflect Paleogene underplating beneath the North China Craton. *Chemical Geology*, *264*, 266–280.

SUPPORTING INFORMATION

Additional Supporting Information may be found online in the supporting information tab for this article.

Table S1 Major element compositions* (wt%) of lower crustal xenoliths from the early Mesozoic igneous rocks in the northern North China Craton.

Table S2 Average compositions (wt%) of minerals* from lower crustal xenolith in early Mesozoic igneous rocks in the North China Craton.

Table S3 Zircon U-Pb-Hfdataforthe Chifeng and Ningcheng igneous rocks and their lower-crustal xenoliths.

Figure S1 Photomicrographs showing the petrography of mafic lower crustal xenoliths from early Mesozoic plutons in the northern part of the North China Craton. a-b, Cpx-granulite xenolith from Chifeng gabbroic diorite; c-d, two-pyroxene granulite xenoliths from Ningcheng quartz-diorite.

Figure S2 U-Pb Concordia diagram for zircons from the Ningcheng quartz-diorite and their xenoliths. The data for diorite NC1140 (a) are from Ma et al. (2016a).

Figure S3 U-Pb Concordia diagram for zircons from the Chifeng gabbroic diorite and their xenoliths.

Figure S4 Plot of zircon εHf(t) versus their U-Pb ages for the Ningcheng quartz-diorite and their xenoliths. Light yellow area (as well as yellow diamonds in a) represents the field of Paleozoic mantle-derived magmas in the northern North China Craton (Zhang *et al.*, 2009a, 2009b, 2009c).

Figure S5 Plot of zircon εHf(t) versus their U-Pb ages for the Chifeng gabbroic diorite and their xenoliths. Light yellow area represents the field of Paleozoic mantle-derived magmas in the northern North China Craton (see Figure S5).

Figure S6 Plots of zircon εHf(t) versus their U-Pb ages for (a) granulite NC1102, (b) Precambrian lower crust and their derivate magmas and in the northern NCC (Jiang et al., 2013 and references therein) and (c) Mesozoic ancient lower crust derived magmas (Yang et al., 2007; Ma et al., 2016b) and regional lower crust (Zheng et al., 2004b) in Liaodong Peninsula in the NCC. These data are used to construct "reworking array" and 176Lu/177Hf of Precambrian basement in the NCC.

How to cite this article: Ma Q, Xu Y-G, Zheng J-P, et al. Phanerozoic magma underplating and crustal growth beneath the North China Craton. *Terra Nova*. 2017;29:211–217. https://doi.org/10.1111/ter.12265